Dynamics of dissolved gas in a cavitating fluid

Igor V. Mastikhin* and Benedict Newling
UNB MRI Centre, Department of Physics, University of New Brunswick, Fredericton, NB E3B 5A3, Canada
(Received 18 September 2008; published 30 December 2008)

A strong acoustic field in a liquid separates the liquid and dissolved gases by the formation of bubbles (cavitation). Bubble growth and collapse is the result of active exchange of gas and vapor through the bubble walls with the surrounding liquid. This paper details a new approach to the study of cavitation, not as an evolution of discrete bubbles, but as the dynamics of molecules constituting both the bubbles and the fluid. We show, by direct, independent measurement of the liquid and the dissolved gas, that the motions of dissolved gas (freon-22, $CHClF_2$) and liquid (water) can be quite different during acoustic cavitation and are strongly affected by filtration or previous cavitation of the solvent. Our observations suggest that bubbles can completely refresh their content within two acoustic cycles and that long-lived (~minutes) microbubbles act as nucleation sites for cavitation. This technique is complementary to the traditional optical and acoustical techniques.

DOI: 10.1103/PhysRevE.78.066316 PACS number(s): 47.55.dp, 47.35.Rs, 61.05.Qr, 62.10.+s

I. INTRODUCTION

The "liquid" we experience in our everyday lives is a symbiotic coexistence of fluids: of the liquid itself, and one or several dissolved gases. A sudden drop in pressure can separate the liquid and the gases by the formation of bubbles, a phenomenon known as cavitation. If such a pressure drop is caused by motion, for example, by a propeller rotating in water, this is a case of hydraulic cavitation, and this is how cavitation was historically discovered [1]. If the pressure drop is produced by strong sound waves, we have an acoustic cavitation. The bubbles grow, oscillate, and eventually collapse producing extreme temperatures and pressures [2–4]. Cavitation can be a highly destructive and chemically active process, so that cavitation is of an immediate importance in science, engineering, and biomedical applications of ultrasound (US).

In acoustic cavitation, bubbles grow during the rarefaction phase, and shrink during the compression phase of the wave. Their collapse and subsequent fragmentation form seeds for new bubbles. Their volume can change by many thousand times between the two extreme states. During the maximum expansion, the partial pressure inside is much lower than that in the surrounding liquid so that dissolved gas and liquid vapor migrate into the bubble. During the phase of maximum compression, the gas, reaction products, and unreacted species are similarly ejected from the bubble.

The violence of collapse is cushioned by the presence of molecules of liquid vapor and formerly dissolved gas in the bubble. Information on the gas dynamics during cavitation is important if cavitation is to be understood and controlled. Commonly used optical and acoustical techniques allow observations of cavitating bubbles at very high detection rates (up to billions of frames per second for photomethods). However, due to their physical nature, these methods cannot provide information on how much of the dissolved gas participates in cavitation, on how long the gas molecules stay inside the bubbles, or on how gas dynamics depend on the number of nucleation sites. Of additional interest is the question of stability of microbubbles that serve as nucleation sites in subsequent sonications [5].

This paper is an attempt to approach cavitation from a different perspective. Instead of looking at cavitation as the evolution of bubbles in the fluid, we look at cavitation from the point of view of the dynamics of the molecules that constitute both the bubbles and the fluid. The best way to get such information is to interrogate the molecules about their experiences in and around the cavitating bubbles. Nuclear magnetic resonance (NMR) promises to accomplish the task: the technique is unaffected by optical and acoustical opacity, and NMR relaxation times, usually much longer than a period of ultrasonic oscillation, can serve as the system memory. The measurement time is on the scale of seconds and minutes, and the obtained information is statistically averaged. This technique is complementary to the traditional optical and acoustical techniques that can provide momentary glimpses into the bubbles' history.

The NMR signal from the liquid phase will overwhelm any signal from the liquid vapor due to a three-orders of magnitude difference in the nuclear magnetic moment (spin) density. The same applies to signal from a dissolved gas if the NMR measurement is performed with the same nucleus. We avoid that problem by dissolving a gas with two atoms of fluorine per molecule (freon-22, $CHClF_2$), enabling us to perform ^{19}F magnetic resonance imaging (MRI) measurements. ^{1}H MRI measurements of water were performed independently.

We measured the dynamics of liquid and dissolved gas during cavitation for two water samples: the filtered water shows a lower cavitation intensity than the unfiltered sample. The results demonstrate that the statistically averaged motion of gas molecules can be quite different from that of the surrounding liquid, depending on the cavitation intensity. Molecules of the dissolved gas enter cavitating bubbles, and their dynamics becomes determined by the dynamics of the cavitation cloud.

*mast@UNB.ca; URL: http://www.unb.ca/physics/mri

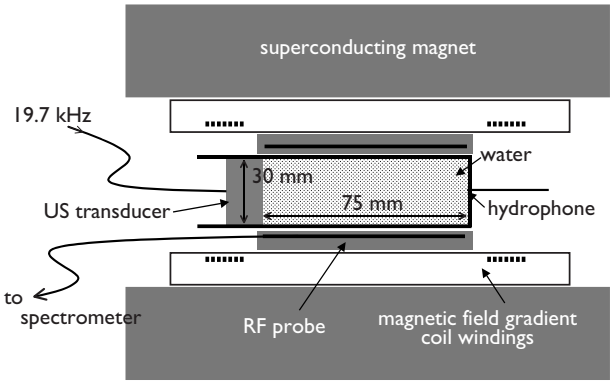

FIG. 1. Schematic of the experimental apparatus.

II. MATERIALS AND METHODS

We employed a horizontal-bore 2.35 T MRI scanner (magnet by Nalorac, CA; Apollo console by TecMag, TX), with homemade 46 mm i.d. ^{1}H and ^{19}F RF quadrature probes. An ultrasonic Langevin-type transducer (SensorTech, ON) was attached to a cylindrical, 30 mm i.d., 75 mm i.l. plastic cuvette filled with water and the dissolved gas. The cuvette was air-tight and positioned inside the magnet horizontally (Fig. 1). Prior to the measurements, highly soluble (0.78. vol/vol [6]) freon-22 was dissolved in water at a constant rate in a semiclosed container for 15 min (by which time the magnetic resonance (MR) signal had reached a constant value, indicating saturation). The freon-22 ^{19}F NMR relaxation time constants T_1 and T_2 change by three orders of magnitude as it is dissolved: from several milliseconds for the free gas [$T_1=T_2=2.1(5)$ ms] to several seconds for the gas dissolved in water [$T_2=1.38(2)$ s and $T_1=2.40(3)$ s].

Two types of water samples were used in the experiments. The first was regular tap water. The second sample was tap water filtered with a 0.2 μm membrane filter (Sarstedt, Germany). The particulate content of both water samples was measured with a laser particle counter (LaserTrac PC2400, ChemTrac Systems Inc, GA); the results are shown in Fig. 2.

Before the start of the NMR measurements, the samples were left in the MRI scanner for 20 min to equilibrate the temperature of the water and gas (initially at 20 °C) with the temperature inside the scanner (15 °C). All NMR measurements were started 30 s after the start of cavitation to give enough time for acoustic streaming patterns to be established

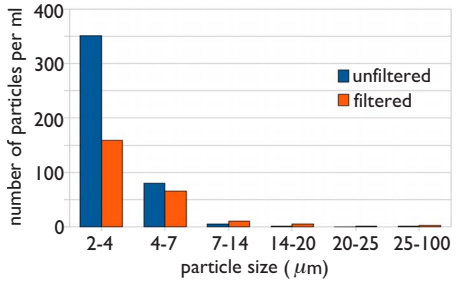

FIG. 2. (Color online) The number of particles per ml of unfiltered and filtered tap water samples measured with a laser particle counter.

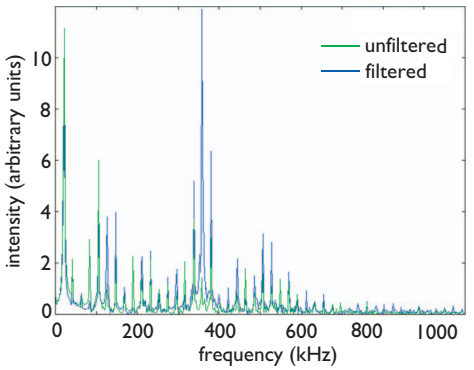

FIG. 3. (Color) Hydrophone data for the two water samples during cavitation at the maximum ultrasound intensity (at an acoustic pressure of 1.6 atm).

[7]. The transducer operated at 19.7 kHz, 1.6 ± 0.05 atm peak-to-peak pressure, with the 1-wavelength standing wave condition for the cuvette. 0.44 W power were absorbed by the water as measured by calorimetry [1.1(2) °C increase in temperature after 10 min of cavitation, measured by a thermocouple].

Before and after a 10-min sonication at the maximum intensity, the ^{19}F NMR spectra of the water samples were acquired on a 500-MHz Varian spectrometer. Neither new ^{19}F-containing compounds nor any change in the freon-22 concentration were detected. A broadband hydrophone (Industrial Sonomechanics, NY) was employed to record acoustic spectra with a spectral width of 5 MHz and a resolution of 2 kHz. The onset of cavitation was detected in the unfiltered water samples at 0.61(4) atm and the filtered water samples at 0.70(4) atm as an increase in harmonics and noise, along with the appearance of subharmonics [8]. The spectra of the acoustic emission at the maximum power are shown in Fig. 3

NMR signal decay following a single pulse of rf excitation [9] were performed with a 40 μs sampling interval, a total acquisition time of 40 ms, and in two regimes: with recovery delays between the consecutive acquisitions of 2.95 s and 10 ms, and with the number of data scans equal to 1 and 64, respectively. A magnetic field gradient spoiler with an amplitude of 4.5 G/cm was applied for 4 ms along the z axis (magnet axis) after each acquisition. The measurements were done in a series of 128, with the ultrasound turned on at No. 20 and turned off at No. 100. The linewidth data were processed with NTNMR (TecMag, TX) by coadding 10 series to improve the signal-to-noise ratio (SNR) and using Lorentzian line fitting for the right line of the doublet.

A standard pulsed-field gradient (PFG) spin echo sequence [9] in 32 gradient steps was used, with a maximum gradient amplitude of 10 G/cm. 8 data scans for a better SNR were performed, with a total imaging time of 7 min. Data were acquired with observation interval, τ, equal to 88 ms. The results are presented, in Sec. III B, as propagators (probability distributions of displacement during the observation interval τ) spatially resolved along the cuvette axis, with displacement Δz as the vertical axis and position along the cuvette z as the horizontal axis (the transducer is positioned at the left at $z=0$ cm). The spatial resolution was

0.5 mm for the ^{1}H data, and 2.2 mm for the ^{19}F data. The measurement duration was limited to 7 min to avoid heating and degassing of water: heating would lead to changes in NMR relaxation parameters, diffusion and gas solubility, and degassing would produce a macroscopic amount of gaseous freon, thus skewing relaxation measurements. Data were Fourier transformed in both the first, spatial and the second, displacement-encoded directions [with the Interactive Data Language (ITT Visual Information Solutions, CO)] and zero-filled once in the second direction. The resulting images were filtered with a 3×3 convolution filter (the new pixel intensity is a result of a summation with intensities of its 8 neighbors, with weights being 16 for the original point and 4 for the 8 others, followed by subsequent normalization). T_2 was measured with a Carr-Purcell-Meiboom-Gill sequence [9], with 0.33 ms echo time, 8192 echoes, 15 s recovery delay, and with 16 scans. The echo centers were collected for fitting. T_1 was measured with an inversion-recovery sequence, with eight inversion delays, eight scans for each. Both relaxation parameters were fitted using the SIGMAPLOT package (Systat Software, Inc., CA). The chemical shift between the center of the doublet line of dissolved Freon and the center of the singlet gaseous Freon was measured as equal to 175.7 Hz (1.77 ppm).

III. RESULTS AND DISCUSSIONS

A. Acoustic and NMR SSFP measurements

The difference in the number of particles available as potential nucleation sites is known to have a direct effect upon cavitation intensity [10] and thus filtering was employed to moderate cavitation. As the results of the particle counting shown in Fig. 2 clearly indicate, the number of particles in the filtered water was reduced significantly compared to that in the unfiltered water. A peristaltic pump with plastic pipes was used to circulate water through the counter and some mechanical attrition of the pipes could contribute to the measured particulate level in the filtered water. Both unfiltered and filtered water samples were bubbled through with the gas, under the same conditions, and then were poured into the clean, air-tight cuvette for the NMR experiments.

The onset of cavitation was detected at a lower acoustic pressure (0.6 atm vs 0.7 atm, see above) in the unfiltered water samples. It is reasonable to assume that the lower tensile strength of the water was caused by the higher number of nucleation sites. The acoustic spectra of the filtered and unfiltered water were different (Fig. 3). A remarkable difference between the two spectra is the appearance of the strong harmonics at higher frequencies, in particular, at and around 360 kHz in the filtered water. A possible explanation of the difference could be a greater presence of free bubbles in the filtered water, contributing to the acoustic excitation. Using the Minnaert formula [11], we can estimate their radii as 7.8–8.8 μm. The hydrophone measurements indicate that a) cavitation begins at lower acoustic pressures in the unfiltered water and b) the cavitation in two water samples proceeds differently.

Our free induction decay (FID) measurements of Freon detected no change in the sample magnetization during cavitation in either of the samples [the first data point of each FID of the freon in the unfiltered sample are shown in Fig. 4(a)]. The Freon spin-spin time constant T_2 showed, almost within experimental accuracy, a slight decrease (see Table I), which was more pronounced in the unfiltered than in the filtered water. After the ultrasound was turned off, the relaxation parameters were found to be slightly lower still.

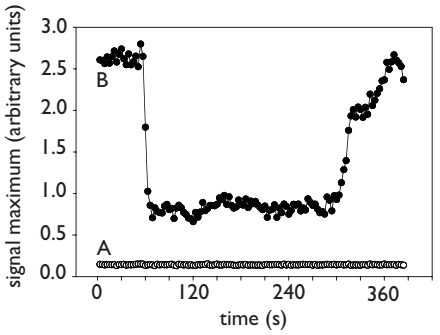

FIG. 4. Two series of 128 free induction decay (FID) measurements of magnetic resonance signal following a single pulse of radiofrequency at 93.2 ^{19}F MHz. The first point only of each FID is shown. The signal was from freon-22 gas ($CHClF_2$) dissolved in unfiltered tap water. Acoustic cavitation occurs between 64 and 320 s. (A) Single measurements separated by 2.95 s. (B) Sets of 64 coadded measurements (40 ms duration), separated by 10 ms intervals; so that the total time for each data point is 3.2 s. The technique in (B) is described as steady-state free precession (SSFP) and these data are strongly affected by cavitation-induced motion (see text).

The dependence of the relaxation parameters on the temperature was measured (see Table II, and was found to be substantial, especially for T_1. Therefore, the slight drop in T_2 of freon could be caused by a combination of the appearance of the gaseous freon and the rising temperature. After the ultrasound was turned off, a local degassing might account for the further decrease in T_2 [no macroscopic bubbles were detected by visual inspection after cavitation inside the scanner; however, macroscopic bubbles could have redissolved in the water by the time ($\sim$1 min) the system is disassembled].

No measurements of T_1 were performed during cavitation due to its higher sensitivity to temperature and the long acquisition time for T_1 measurements (at least 16 min, twice as long as the usually employed cavitation/MRI measurement time.)

Neither the amount of nuclear magnetization, nor its spin-spin relaxation properties were significantly affected by cavitation. When polarized (at thermal equilibrium) nuclear spins

TABLE I. T_2 and the linewidth of freon-22 dissolved in unfiltered and filtered water before, during, and after the application of ultrasound at maximum power (1.6 atm acoustic pressure).

	Before	During	After
T_2/s, unfiltered	1.385(18)	1.35(18)	1.340(17)
T_2/s, filtered	1.389(20)	1.376(18)	1.373(18)
Linewidth/Hz, unfiltered	48.8(4)	43.9(4)	51.0(5)
Linewidth/Hz, filtered	39.9(4)	43.3(4)	40.1(4)

TABLE II. T_2 and T_1 of freon-22 dissolved in the unfiltered water vs temperature.

T/°C	15	20	23	25	26.5	29	31	35
T_2	1.38(2)	1.211(8)	1.144(7)	1.186(5)	1.19(1)	1.01(1)	0.84(2)	0.835(16)
T_1	2.40(3)	3.09(3)	3.45(4)					

of ^{19}F in freon molecules enter cavitating bubbles, one could hypothesize that high temperatures inside might destroy nuclear magnetization; however, it is known that only a small fraction of cavitating bubbles collapse violently [11]. Therefore, it was unlikely that a substantial number of freon molecules would experience extreme cavitation conditions, and unlikely that much nuclear magnetization would be destroyed.

However, when we reduced the delay between repeats of the FID measurement from 2.95 s to 10 ms, turning the FID into a steady-state free precession (SSFP) NMR measurement, the difference between cavitating and noncavitating FIDs became substantial [Fig. 4(b)]. The observed differences also depended on the type of water: filtered vs unfiltered. The SSFP measurement is highly sensitive to changes in relaxation times (which were very minor, see above) and to the presence of motion [12], to which it was sensitized by an addition of the spoiler gradient along the z direction. We conclude that cavitation-induced motion is responsible for the signal attenuation observed in Fig. 4(b) (and, therefore, Fig. 5, below).

The 128 series of SSFP magntiude spectra (obtained from the FID by Fourier transformation) for the unfiltered and filtered water samples are presented in Fig. 5, with ultrasound turned on at No. 20 and off at No. 100. The series are plotted starting from the top right corner of each spectrum. The doublet lines belong to the dissolved freon. The location of the broad line of the gaseous freon, which we had hoped to detect, is indicated by the vertical arrows at 1.77 ppm

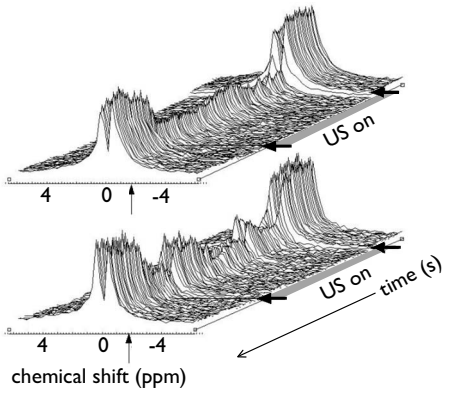

FIG. 5. Magnitude spectra produced by the Fourier transformation of the full FIDs represented in Fig. 4(b). Upper spectra were obtained from unfiltered water, lower spectra were obtained from filtered water. The doublet spectra are characteristic of Freon dissolved in water. The vertical arrows indicate the position on the chemical shift axes which would be occupied by the broad singlet line of gaseous freon: this line is not observed, however, even during cavitation (see text). The ultrasound transducer is turned on at the 20th (64 s) and off at the 100th (320 s) NMR measurement.

from the centre of the doublet. The original intention of rapid pulsing (every 10 ms) in the experiments was to utilize the difference in T_1 relaxation between the dissolved and gaseous freon: while the dissolved freon's lines would be saturated, the gaseous freon's line, if present, would remain unaffected. If the transverse magnetization between the pulses is completely destroyed by the spoiler gradient, then the signal amplitude $S(t)$, due to a species of particular T_1, will obey the well-known formula

$$S(t) = S(0)\sin\alpha\frac{1-E_1}{1-\cos\alpha E_1}, \tag{1}$$

where $E_1=\exp(-\mathrm{TR}/T_1)$ and TR=50 ms is the time between the start of each measurement [13,14]. The total signal detected is, therefore, a sum of contributions from different species (in the present case gaseous and dissolved freon), weighted according to Eq. (1) by their different T_1. For T_1 of dissolved freon equal to 2.4 s, with the flip angle $\alpha=90°$, the attenuation of the dissolved freon line would be by a factor of 52.6. However, the transverse magnetization is not completely destroyed in our experiments, as is clear from the continued domination of the spectrum by the dissolved-freon doublet. In this case, the steady-state signal is determined by an interaction of overlapping transverse magnetizations from the previous pulses. Since the spolier gradient is uncompensated, and without incorporation of the motion effects, we can express the signal as

$$S(t) = S(0)\sin\alpha\frac{1-E_1}{C}\left[\frac{C+DE_2}{\sqrt{D^2-C^2}}-E_2\right]. \tag{2}$$

Here $E_2=\exp(-\mathrm{TR}/T_2)$, $C=E_2(E_1-1)(1+\cos\alpha)$, $D=(1-E_1\cos\alpha)-(E_1-\cos\alpha)E_2^2$ (see Ref. [15] for an excellent review). The signal essentially depends on the combination of relaxation parameters which give us an attenuation factor of 3.48. The experimentally measured attenuation factors for quiescent water were 3.97 and 4.15 for the unfiltered and the filtered water, respectively. No line of the gaseous freon was detected during cavitation in either of the samples. Our inference from this observation is limited by the signal-to-noise ratio (SNR) of 22. Including the attenuation factor as 4, we estimate an upper limit to the free-to-dissolved gas mass ratio of 1.1%.

The dissolved freon linewidths narrowed during cavitation in the unfiltered water, and broadened in the filtered water (see Table I). It is relevant to note that the measured linewidth is determined by the magnetic field inhomogeneity across our sample (0.4 ppm), and our spectral resolution is 25 Hz. In cavitation, we can expect two effects on the linewidth. Motion of the spins can result in the averaging of the field during the acquisition (as was observed in Ref. [16]) and thus narrowing of the lines. The presence of the bubbles,

on the other hand, introduces local field inhomogeneity and thus will result in line broadening. The efficiency of the former depends on the average speed of spins, and of the latter depends on the proximity of the spins to the bubbles and the average bubble population in terms of both density and radius. The observed narrowing is most likely caused by the averaging of the field in the course of cavitation-induced motion. Averaging will be more efficient if spins move slowly all the time, than if they move rapidly during only a fraction of the time.

Temporal behavior of the signal in the two samples was also different. As soon as the ultrasound is turned on at scan No. 20, the line intensity in the unfiltered water drops and reaches a "steady state" by No. 22 (6.4 s from the start). In the filtered water, the line intensity decreases more slowly and reaches the steady state by No. 24 (12.8 s). This is further evidence of the motion-induced signal attenuation. As soon as the ultrasound is on, cavitation propagates along the vessel. At such low frequencies as 20 kHz, water absorption is negligible, and acoustic streaming caused by water absorption will not develop, unless the water cavitates. In tests with thoroughly degassed water, no motion of water (no signal attentuation) was detected. It is the appearance of cavitating bubbles that leads to the macroscopic motion of both gas and the liquid. The more spins are involved in cavitation, the further they move along the direction of the magnetic field gradient, and the more portions of magnetization accumulated from previous pulses interfere destructively, resulting in the signal drop. The propagation speed depends on the cavitation intensity [7].

Lastly, the intensity during cavitation remains at about the same level in the unfiltered water while it fluctuates substantially in the filtered water in the interval of 32–40 s. Such behavior indicates unstable motion in the filtered water.

B. Pulsed field gradient (PFG) measurements

The SSFP signal is determined by several factors in a complicated manner, and the sequence usually is employed as a qualitative technique. For quantitative, spatially resolved measurements, we performed PFG measurements of both water and dissolved gas motion during cavitation. The PFG experiment measures an average displacement (Δz) during the time interval (τ) between two gradient pulses; that displacement is often interpreted in terms of an average velocity ($\Delta z/\tau$) for steady flows [9]. For an ensemble of spins, with potentially different motion histories, the PFG measurement yields a distribution of such temporally averaged displacements across the ensemble.

PFG measurements of water motion showed that the displacement was comparable in the unfiltered and filtered water [Figs. 6(a) and 6(b)], with active circulation taking place. The region near the transducer, where cavitation is the strongest, exhibits greater motion than the rest of the cuvette.

Measurements of gas motion showed a different picture, with dynamics uncoupled from that of the liquid [Figs. 6(c) and 6(d)]. In the unfiltered water [Fig. 6(c)], the displacement in the region near the transducer is of the same order as in the absence of cavitation (not shown). Gas and liquid dynamics are uncoupled because of the presence of developed cavitation: a substantial portion of gas participates in the bubble motion, which is governed by gradients of acoustic pressure in the standing wave and interactions between the bubbles, particularly near the transducer.

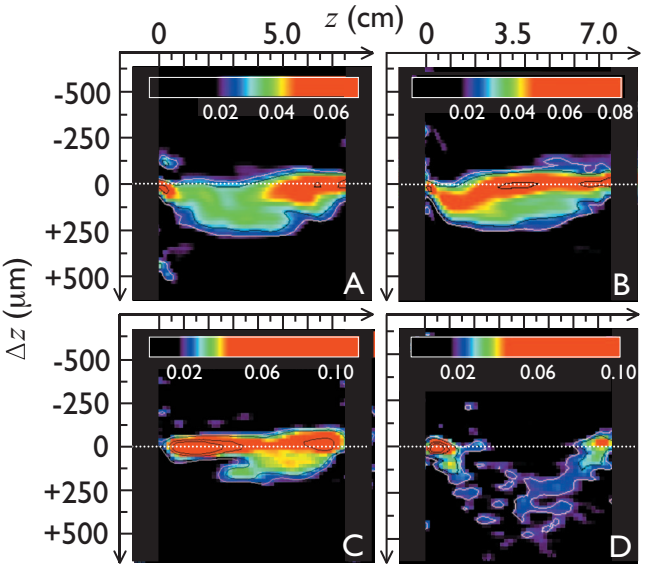

FIG. 6. (Color) Maps of displacement (Δz) vs position along the cuvette (z) for (A),(B) the ^{1}H in the solvent (water) and (C),(D) ^{19}F in the solute (freon-22, $CHClF_2$). All displacements occur during an interval of τ=88 ms while acoustic cavitation was taking place. Maps are shown for both (A),(C) unfiltered tap water and (B),(D) tap water treated using a 0.2 μm filter. In each propagator map, the color at each position indicates the probability of that particular displacement (vertical axis) at that particular location in the cuvette (horizontal axis) occurring during the 88 ms of observation. The total probability is normalized to one at each z. The white contour is at a probability of 0.023 in all maps. Other (black) contours show probabilities of 0.03, 0.06, and 0.08. The acoustic transducer is to the left, at z=0 cm. The end of the cuvette is at z=7.5 cm. Noise outside this region has been set to zero. Positive displacements are away from the transducer.

It is also seen that the dynamical behaviour of gas in filtered and unfiltered water (in which the cavitation is more intense) is very different. Except for the regions close to the cuvette ends, there is no stationary gas at all in filtered water: within the τ=88 ms interval, almost all gas molecules in the cuvette are substantially displaced. The gas propagator forms an arc pattern with displacements greater than those of gas in the unfiltered water. Most unexpectedly, for the filtered water, displacements of the gas are greater than displacements of the water itself, around 380 μm in the direction away from the transducer, at the center of the cuvette. The motion of gas in the unfiltered water, on the other hand, is localized next to the transducer where cavitation is the strongest, and its displacement is smaller than that of surrounding water. Figure 7 shows profiles, along the cuvette, of the quantity of stationary dissolved gas [extracted from Figs. 6(c) and 6(d)]. This emphasizes that the less intense cavitation in the filtered water is associated with a generally greater motion of the gas molecules.

One possible explanation of these observations for the filtered water is that the gas molecules move faster than wa-

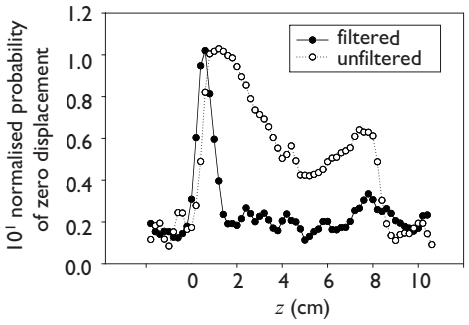

FIG. 7. Profiles of the probability that freon-22 be stationary, taken along the dotted lines in Fig. 6(c) for unfiltered water and Fig. 6(d) for filtered water. In the filtered water, in which cavitation is less intense, a much greater fraction of the dissolved gas is disturbed by acoustic cavitation.

ter because their travel is mediated by the cavitating bubbles. Due to weaker cavitation in the filtered water, cavitating bubbles do not interact much with each other, making it possible for them to travel quite far. In a dense cavitation cloud, as in the unfiltered water with many impurities, cavitating bubbles actively interact with each other so they cannot move very far. It is also well known from theory [17] that rapid changes in bubble volume limit the amount of gas involved in cavitation to that dissolved in the boundary layer of the liquid around the bubbles. If the surrounding liquid can be refreshed by, for example, induced motion, the gas exchange between the bubble and the environment is enhanced [11]. The moving bubbles act as nucleation sites, spawning new bubbles and involving most of the dissolved gas in cavitation. This picture resembles a superheated liquid that begins to boil as soon as nucleation sites are added to the system. The absolute volume of water involved in bubble motion might be of the same order as that of gas; however, since it represents less than 1/1000 of the volume of quiescent water, its displacement goes unnoticed.

We would not like to claim that this relationship between dissolved-gas and water motions is general. In fact, the interplay of gas and water motions depends, at the very least, on both the ultrasound intensity and the cavitation activity. One can expect that a higher ultrasound intensity and, therefore, higher acoustic pressure will yield bubble motion which is strongly controlled by the gradients of acoustic pressure (primary Bjerknes forces) so that the well-known node-antinode bubble migration in the standing wave [11] will be dominant. The transducer employed herein could not operate at higher intensities, so we performed the same measurements with a different transducer at much higher acoustic pressures (up to 7 atm), and found certain intensities at which the motion of gas in the filtered water was greater than in the unfiltered. At the same time, gas motion was much smaller than the motion of the surrounding liquid, again indicating a very strong distinction between motion of the species during cavitation. The measurements were done with a different experimental setup and a transducer type (an acoustic horn [18]) and will be reported in detail elsewhere. However, it is clear that using NMR to probe the dissolved-gas and water motions gives a unique viewpoint from which to examine the onset of cavitation.

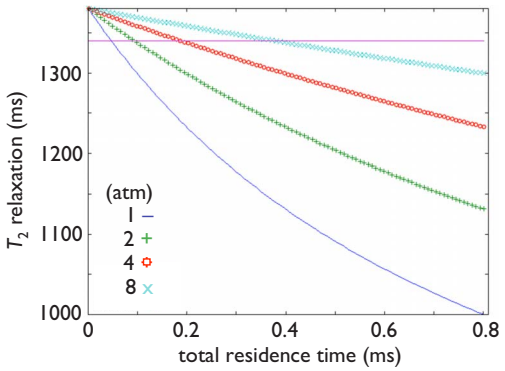

FIG. 8. (Color online) The expected T_2 relaxation time constant as a function of the total residence time and average pressure inside the bubbles, as estimated by the two-site exchange model [Eq. (3) and accompanying text]. T_2=1350 ms before cavitation; the horizontal line at T_2=1340 ms indicates the observed value of T_2 during cavitation. The curves correspond to estimates of the change in observed T_2 at (solid line) 1 atm, (+) 2 atm, (□) 4 atm, and (×) 8 atm.

In light of these PFG displacement measurements, we recall that relaxation measurements do not show a measurable difference between quiescent and cavitating water (either filtered or unfiltered), within the accuracy of our measurement (3.7%). PFG demonstrates that there is no stationary gas in filtered water during cavitation, most of it moves with the bubbles, which are gaseous objects. The ^{19}F T_2 relaxation time constant of freon in the gaseous state is 2 ms, but this is not reflected in the T_2 during cavitation. Therefore, the total time which gas molecules spend inside the bubbles, as free gas, must be much shorter than around 1 ms over the course of our T_2 measurement (3 s). (We use the term"total time" to mean the total amount of time gas molecules spend in the gaseous phase during the measurement, which may include many entries of and exits from the bubbles.)

To estimate the total residence time, we used a two-site exchange model [19,20]. In the model, the observed relaxation rate $1/T_2$ equals the weighted average of the relaxation rates of the spins in dissolved state $1/T_{2d}$ and gaseous state $1/T_{2g}$:

$$\frac{1}{T_2} = \frac{X_d}{T_{2d}} + \frac{X_g}{T_{2g} + \tau_g}, \tag{3}$$

where τ_g is the residence time of the spins in the gaseous state, and X_d and X_g are fractions of nuclear magnetization, with $X_d + X_g = 1$. The fractions then are estimated as equilibrium magnetizations of the two states in the first-order reversible reaction $X_g/X_d = k_1/k_{-1}$, where k_1 and k_{-1} are kinetic rate constants [3]. k_{-1} is evaluated as $1/\tau_g$. From the PFG measurements, it is known that most of the dissolved gas comes into contact with cavitating bubbles within 88 ms, giving us an upper limit for $k_1 = 11.4\ \mathrm{s}^{-1}$. The resulting value of $\tau_g < 100\ \mu$s is found with a conservative choice of $k_1 = 1\ \mathrm{s}^{-1}$ under the condition that the observed value of T_2 changes from 1.38 s to 1.34 s (see Fig. 8). The total time of 100 μs equals two oscillation periods of the acoustic wave. With the maximum displacement around 0.38 mm (Fig. 6),

that gives 3.8 m/s as a low limit for the bubbles highest speeds.

If we fix the total residence time at 0.1 ms, the estimate of the gaseous population X_d will be equal to 0.01%, which can explain why no signal from gaseous Freon was detected: such a small amount is below the sensitivity limits of the NMR equipment used in the experiments.

The proposed phenomenological two-site exchange model depends heavily on relaxation parameters that can increase with pressure, due to spin-rotational mechanisms [21,22]. The intervals of extreme pressure inside collapsing bubbles occupy only a small fraction of the acoustic period. For most of the period the bubble gases are at atmospheric or lower pressures. If the bubbles are very small, the surface tension inside will increase the pressure according to the Young-Laplace equation

$$P_i = P_o + \frac{2\gamma}{R}. \tag{4}$$

P_i and P_o are the pressures inside and outside the bubble, γ is the surface tension, and R is the bubble radius.

We performed measurements of the T_2 of gaseous freon-22 vs pressure that showed a doubling of T_2 as the pressure increased to 2 atm, still staying within the millisecond range. The plots in Fig. 8 show the elongation of the total residence time for T_2s corresponding to 1, 2, 4, and 8 atmospheres (the last value was extrapolated from the experimental data).

Two atmospheres of pressure would correspond to a gaseous bubble with a radius of 1.44 μm. Further relaxation mechanisms are important to the gas molecule inside a submicrometer bubble. Interactions with both other gas molecules and the walls of the bubble, can cause a change in NMR relaxation times. The observed massive displacement of gas molecules is unlikely to proceed in very small bubbles due to the increasing importance of drag force ($\propto$ area) over acoustic force ($\propto$ volume) with decreasing size. However, we have no information on the relative populations of submicrometer-sized and larger bubbles at any instant during cavitation. The acoustic spectra do indicate a large presence of bubbles in the 8 μm range, corresponding to Young-Laplace pressures close to atmospheric.

Another piece of evidence of the short total residence time of gas molecules inside cavitating bubbles is the absence of line broadening during cavitation. Local magnetic field gradients caused by the magnetic susceptibility difference between the gaseous bubble and water would be reflected in the FID data as a shortening of the signal lifetime. This effect would be proportional to the average residence time of the gas molecule in the vicinity of a bubble. Since we have not detected any substantial change in the dissolved gas linewidth, we conclude that either this mechanism is not present, or the residence time is, again, <1 ms.

When we repeated the measurements after a 2 min delay, we found that the propagators for gas in filtered water began to strongly resemble those in the unfiltered water [Figs. 9(a), cf. Fig. 6(c)]: there was no arc of displacements, and there was a substantial amount of the stationary gas. After a one-hour delay, propagators only partially recovered to their original shape [Fig. 9(b), cf. Fig. 6(d)]. Propagators for water exhibited the same tendency, with motion becoming more violent both in the filtered and the unfiltered water. This is an indication of an increased number of nucleation sites that lead to a cavitation enhancement. Since the filtered water does not have many impurities, the only possible source of an increase in nucleation sites is microbubbles left after the previous cavitation event. A further indication of the presence of seeding microbubbles is a slight decrease in T_2 after the ultrasound was turned off. Contrary to general theoretical considerations that estimate microbubble lifetime on the order of seconds [23,24], their measured stability is remarkable. It is possible that, in our experiments, microbubbles were temporarily stabilized by the plastic surface of the vessel walls.

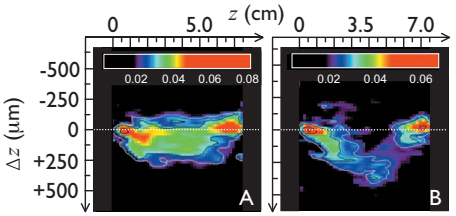

FIG. 9. (Color) Maps of freon-22 displacement in filtered water during second and third acoustic cavitation events (A) two minutes after the first cavitation [Fig. 6(d)] and (B) one hour after the second cavitation.

IV. CONCLUSION

MRI provides statistically averaged information on molecular dynamics of both liquid and gaseous phases and dissolved gas species of cavitation and, as such, can serve as a method complementary to the optical and acoustical techniques traditionally employed in cavitation research. The behavior of molecules of the liquid (water) and dissolved gas (freon-22) during acoustic cavitation was investigated in this work.

We have found that gas and liquid dynamics during acoustic cavitation can be completely uncoupled, depending on the number of nucleation sites. One of the remarkable results was a very active engagement of the dissolved gas in the cavitation: during our observation window of 88 ms, most of the gas molecules in the vessel moved faster than the surrounding liquid. No line of the gaseous freon was detected with the spectroscopic measurements, giving an estimate of the total amount of freon in the gaseous phase less than 1.1%. There was also no noticeable change in the T_2 relaxation. Based on these observations, we estimate the total time for gas molecules inside cavitating bubbles is on the order of, or less than, 100 μs, meaning that gas content within bubbles is refreshed within two oscillation periods. The estimate is strongly suggestive of bubble dynamics in which each new position of a fully expanded bubble involves a different collection of gas molecules than that of the previous cycle.

There are several factors that can potentially modify NMR relaxation parameters. The elevated pressure and

surface-volume effects in submicron bubbles can affect spin interactions leading to longer T_1 and T_2 and making the estimate of the total residence time longer. Another unknown factor is the presence of water vapor in the bubbles. Cavitation studied as a temporarily porous medium represents a substantial challenge, and more NMR research in this field is necessary.

The very high solubility of freon-22 undoubtedly influenced the dynamics of the gas in and around the cavitating bubbles, most likely reducing the residence time inside the bubbles to a minimum. Even with this high solubility, our measurements were performed at the sensitivity limits. Substitution of a gas, or a series of gases, with lower solubility will allow the gas molecules to stay longer inside the bubbles and thus will be an exciting opportunity to probe the gas dynamics, provided challenges associated with lower gas concentrations and corresponding lower sensitivity can be overcome.

Microbubbles remaining after cavitation events can be very stable, influencing cavitation dynamics significantly after 2 min delays, but minimally after one hour delays between the events. This information is pertinent to clinical ultrasound applications where the control of cavitation activity is required.

ACKNOWLEDGMENTS

The authors gratefully acknowledge financial support from the Natural Science and Engineering Council of Canada and the Harrison McCain Foundation (B.N.). We thank Murray Olive and Brian Titus for fabricating parts of the experimental setup. Thanks also to Dr. L. Calhoun, who acquired high-resolution NMR spectra of the dissolved Freon and to Eric Bell, who helped with the particle count measurements. The UNB MRI Centre is supported by NSERC.

[1] F. R. Young, *Cavitation* (CRC Press, Boca Raton, 1990).
[2] E. B. Flint and K. S. Suslick, Science **253**, 1397 (1991).
[3] D. J. Flannigan and K. S. Suslick, Nature (London) **434**, 52 (2005).
[4] D. F. Gaitan, L. A. Crum, C. C. Church, and R. A. Roy, J. Acoust. Soc. Am. **91**, 3166 (1992).
[5] C. C. Church, Ultrasound Med. Biol. **28**, 1349 (2002).
[6] *Gas Encyclopædia*, 2nd ed. (Air Liquide, Amsterdam, 1992).
[7] I. V. Mastikhin and B. Newling, Phys. Rev. E **72**, 056310 (2005).
[8] E. Cramer and W. Lauterborn, Appl. Sci. Res. **38**, 209 (1982).
[9] P. T. Callaghan, *Principles of Nuclear Magnetic Resonance Microscopy* (Oxford University Press, Oxford, UK, 1991).
[10] A. A. Atchley and A. Prosperetti, J. Acoust. Soc. Am. **86**, 1065 (1989).
[11] T. G. Leighton, *The Acoustic Bubble* (Academic Press, Amsterdam, Netherlands, 1997).
[12] S. Patz and R. C. Hawkes, Magn. Reson. Med. **3**, 140 (1986).
[13] P. Brunner and R. R. Ernst, J. Magn. Reson. (1969-1992) **33**, 83 (1979).
[14] J. S. Waugh, J. Mol. Spectrosc. **35**, 298 (1970).
[15] M. Vlaardingebroek and J. den Boer, *Magnetic Resonance Imaging*, 2nd ed. (Springer, Berlin, Germany, 1999), Chap. 4.
[16] J. Homer and M. J. Howard, Ultrason. Sonochem. **5**, 141 (1999).
[17] M. M. Fyrillas and A. J. Szeri, J. Fluid Mech. **277**, 381 (1994).
[18] S. L. Peshkovsky and A. S. Peshkovsky, Ultrason. Sonochem. **14**, 314 (2007).
[19] R. A. Dwek, *Nuclear Magnetic Resonance in Biochemistry* (Clarendon Press, Oxford, UK, 1973), pp. 37–47.
[20] B. W. Dubois and A. S. Evers, Biochemistry **31**, 7069 (1992).
[21] P. J. Prado, B. J. Balcom, I. V. Mastikhin, A. R. Cross, R. L. Armstrong, and A. Logan, J. Magn. Reson. **137**, 324 (1999).
[22] D. O. Kuethe, T. Pietrass, and V. Behr, J. Magn. Reson. **177**, 212 (2005).
[23] A. Kabalnov, D. Klein, T. Pelura, E. Schutt, and J. Weers, Ultrasound Med. Biol. **24**, 739 (1998).
[24] P. S. Epstein and M. S. Plesset, J. Chem. Phys. **18**, 1505 (1950).